



Fermi National Accelerator Laboratory

FERMILAB-Pub-98/193-T

**QCD Corrections to Spin Correlations in Top Quark Production at
Lepton Colliders**

Jiro Kodaira and Takashi Nasuno

*Department of Physics, Hiroshima University
Higashi-Hiroshima 739-8526, Japan*

Stephen Parke

*Fermi National Accelerator Laboratory
P.O. Box 500, Batavia, Illinois 60510*

July 1998

Submitted to *Physics Letters B*

Disclaimer

This report was prepared as an account of work sponsored by an agency of the United States Government. Neither the United States Government nor any agency thereof, nor any of their employees, makes any warranty, expressed or implied, or assumes any legal liability or responsibility for the accuracy, completeness, or usefulness of any information, apparatus, product, or process disclosed, or represents that its use would not infringe privately owned rights. Reference herein to any specific commercial product, process, or service by trade name, trademark, manufacturer, or otherwise, does not necessarily constitute or imply its endorsement, recommendation, or favoring by the United States Government or any agency thereof. The views and opinions of authors expressed herein do not necessarily state or reflect those of the United States Government or any agency thereof.

Distribution

Approved for public release; further dissemination unlimited.

QCD Corrections to Spin Correlations in Top Quark Production at Lepton Colliders

JIRO KODAIRA AND TAKASHI NASUNO

*Dept. of Physics, Hiroshima University
Higashi-Hiroshima 739-8526, JAPAN*

AND

STEPHEN PARKE

*Theoretical Physics Department
Fermi National Accelerator Laboratory
P. O. Box 500, Batavia, IL 60510, USA*

Abstract

Spin correlations, using a generic spin basis, are investigated to leading order in QCD for top quark production at lepton colliders. Eventhough, these radiative corrections induce an anomalous γ/Z magnetic moment for the top quarks and allow for single, real gluon emission, their effects on the top quark spin orientation are very small. The final results are that the top (or anti-top) quarks are produced in an essentially unique spin configuration in polarized lepton collisions even after including the $\mathcal{O}(\alpha_s)$ QCD corrections.

PACS number(s): 12.38.Bx, 13.88.+e, 14.65.Ha

hep-ph/9807209
July 1998

1 Introduction

The discovery of the top quark, with a mass near 175 GeV [1, 2], provides us with a unique opportunity to better understand electro-weak symmetry breaking and to search for hints of physics beyond the standard model. It has been known for sometime that top quarks decay electroweakly before hadronization [3, 4] and that there are significant angular correlations between the decay products of the top quark and the spin of the top quark [5]. Therefore if the production mechanism of the top quarks correlates the spins of the top and anti-top quarks, there will be a sizable angular correlations between all the particles, both incoming and outgoing, in these events.

There are many papers on the angular correlations for top quark events [6, 7] produced both at e^+e^- colliders [8] and hadron colliders [9]. In most of these works, the top quark spin is decomposed in the helicity basis. Recently, Mahlon and Parke [10] have proposed a more optimal decomposition of the top quark spin which results in a large asymmetry at hadron colliders. Parke and Shadmi [11] extended this study to e^+e^- annihilation process at the leading order in the perturbation theory and found that the “off-diagonal” basis is the most efficient decomposition of the top (anti-top) quark spin. In this spin basis the top quarks are produced in an essentially unique spin configuration. Since this result is of great interest, it is of crucial importance to estimate the radiative corrections to this process which are dominated by QCD effects.

The QCD corrections to top quark production can be calculated perturbatively at energies sufficiently above the production threshold of the top quark pairs. The analytical study of QCD radiative corrections to heavy quark production was pioneered in Ref. [12] (see *e.g.* Ref. [13] for a recent article). Polarized heavy quark production, in the helicity basis, has also been investigated by many authors [14, 15].

In this article, we present an analytic differential cross section for polarized top quark production at the QCD one-loop level. We focus on the issue of what is the

optimal decomposition of the top quark spin for e^+e^- colliders *. We have calculated the cross section in a “generic” spin basis which includes the helicity basis as a special case. The radiative corrections, in general, add two effects to the Born level analysis: the first is that a new vertex structure (anomalous γ/Z magnetic moment) is induced by the loop corrections to the tree level vertex, the second is that a (hard) real gluon emission from the final quarks can flip the spin and change the momentum of the parent quarks. Therefore, compared to the radiative corrections of physical quantities which are spin independent, it is possible that spin-dependent quantities maybe particularly sensitive to the effects of QCD radiative corrections.

The article is organized as follows. In Section 2, we examine the QCD corrections to the polarized top (anti-top) quark production in the soft gluon approximation. The aim of this section is: (1) we estimate the numerical effects from the new vertex structure on the spin correlation found in the Born level analysis and (2) we show that we can use the off-diagonal basis as a optimal basis also at the QCD one-loop level. In Section 3, we present our analytic calculations of the full one-loop corrections to the polarized top quark production in a generic spin basis. We give the numerical results both in the helicity, beamline and the off-diagonal bases in Section 4. Here we compare the full one loop results with those of the Born and soft gluon approximations. Finally, Section 5 contains the conclusions. The phase space integrals which are needed in Section 4 are summarized in Appendix A. The unpolarized total cross section for top pair production, using our results, is given in Appendix B as a cross check.

* The physics of top quark production at muon colliders and e^+e^- colliders is identical provide the energy is not tuned to the Higg boson resonance.

2 Spin Correlations in the Soft Gluon Approximation

In this section we derive the first order QCD corrected spin dependent, differential cross section for top quark pair production in the soft gluon approximation. It is instructive to first consider the soft gluon approximation because in this approximation only the QCD vertex corrections modify the spin correlations of the top quarks. The full one-loop analysis will be given in the next section. We use the same generic spin basis as in Ref. [11]. In this paper we do not consider transverse polarization of the top quarks [†] since we are interested in how QCD corrections modify the tree level spin correlations and which spin basis is the most effective for spin correlation studies. Therefore we use a generic spin basis with the spin of the top quark and anti-top quark in the production plane. We define the spins of the top and anti-top quarks by the parameter ξ as given in Fig.1.

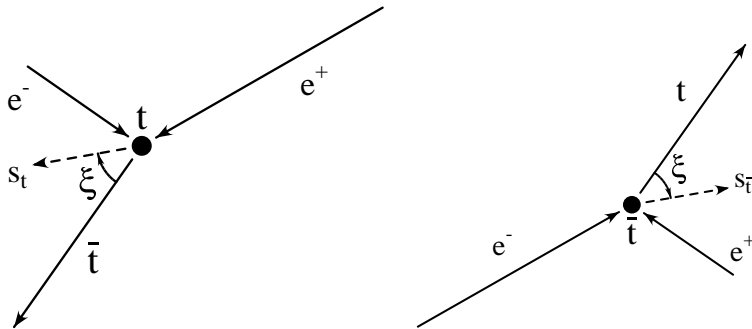


Figure 1: The generic spin basis for the top (anti-top) quark in its rest frame. \mathbf{s}_t ($\mathbf{s}_{\bar{t}}$) is the top (anti-top) spin axis.

The top quark spin is decomposed along the direction \mathbf{s}_t in the rest frame of the top quark which makes an angle ξ with the anti-top quark momentum in the clockwise

[†]It is known [7] that the transverse top quark polarization becomes nonzero when the higher order QCD corrections are included and that this transverse polarization is very important and related to the phenomena of CP violation.

direction. Similarly, the anti-top quark spin states are defined in the anti-top rest frame along the direction $\mathbf{s}_{\bar{t}}$ having the same angle ξ from the direction of the top quark momentum. We use the following notation in this paper: the state $t_{\uparrow}\bar{t}_{\uparrow}(t_{\downarrow}\bar{t}_{\downarrow})$ refers to a top with spin in the $+\mathbf{s}_t(-\mathbf{s}_t)$ direction in the top rest frame and an anti-top with spin $+\mathbf{s}_{\bar{t}}(-\mathbf{s}_{\bar{t}})$ in the anti-top rest frame.

The one-loop QCD correction to the cross section is given by the interference between the tree and one-loop vertex diagrams in Fig.2.

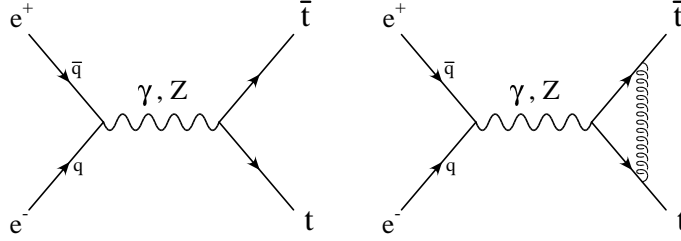


Figure 2: The Born and the QCD one-loop contributions to the $e^-e^+ \rightarrow t\bar{t}$ process.

At the one-loop level, the $\gamma - t - \bar{t}$ and $Z - t - \bar{t}$ vertex functions can be written in terms of three form factors A, B, C as follows:

$$\Gamma_{\mu}^{\gamma} = \epsilon Q_t \left[(1 + A) \gamma_{\mu} + B \frac{t_{\mu} - \bar{t}_{\mu}}{2m} \right], \quad (1)$$

$$\begin{aligned} \Gamma_{\mu}^Z = \frac{\epsilon}{\sin \theta_W} & \left[\{ Q_t^L (1 + A) + (Q_t^L - Q_t^R) B \} (\gamma_L)_{\mu} \right. \\ & + \{ Q_t^R (1 + A) - (Q_t^L - Q_t^R) B \} (\gamma_R)_{\mu} \\ & \left. + \frac{Q_t^L + Q_t^R}{2} B \frac{t_{\mu} - \bar{t}_{\mu}}{2m} + \frac{Q_t^L - Q_t^R}{2} C \frac{t_{\mu} + \bar{t}_{\mu}}{2m} \gamma_5 \right], \quad (2) \end{aligned}$$

where $Q_t = \frac{2}{3}$ is the electric charge of the top quark in units of the electron charge ϵ , θ_W is the Weinberg angle, and m and $t_{\mu}(\bar{t}_{\mu})$ are the mass and the momentum of the top (anti-top) quark ($\gamma_{R/L}^{\mu} \equiv \gamma^{\mu} \frac{1 \pm \gamma_5}{2}$). The top quark couplings to the Z boson are given by

$$Q_t^L = \frac{3 - 4 \sin^2 \theta_W}{6 \cos \theta_W}, \quad Q_t^R = -\frac{2 \sin^2 \theta_W}{3 \cos \theta_W}. \quad (3)$$

After multiplying the wave function renormalization factor (we employ the on-shell renormalization scheme), the “renormalized” form factors read

$$A = \hat{\alpha}_s \left[\left(\frac{1+\beta^2}{\beta} \ln \frac{1+\beta}{1-\beta} - 2 \right) \ln \frac{\lambda^2}{m^2} - 4 + 3\beta \ln \frac{1+\beta}{1-\beta} \right. \\ \left. + \frac{1+\beta^2}{\beta} \left\{ \frac{1}{2} \ln^2 \frac{1+\beta}{1-\beta} + \ln^2 \frac{1+\beta}{2\beta} - \ln^2 \frac{1-\beta}{2\beta} + 2\text{Li}_2 \left(\frac{1-\beta}{1+\beta} \right) + \frac{2}{3}\pi^2 \right\} \right], \quad (4)$$

$$B = \hat{\alpha}_s \frac{1-\beta^2}{\beta} \ln \frac{1+\beta}{1-\beta}, \quad (5)$$

$$C = \hat{\alpha}_s \left[(2+\beta^2) \frac{1-\beta^2}{\beta} \ln \frac{1+\beta}{1-\beta} - 2(1-\beta^2) \right], \quad (6)$$

where β is the speed of the produced top (anti-top) quark and the strong coupling constant is $\hat{\alpha}_s \equiv \frac{C_2(R)}{4\pi} \alpha_s = \frac{C_2(R)}{(4\pi)^2} g^2$ with $C_2(R) = \frac{4}{3}$ for SU(3) of color. We have introduced an infinitesimal mass λ for the gluon to avoid infrared singularities. In the above expressions, we have shown only the real part of the form factors because (1) the Z width is negligible in the region of center-of-mass (CM) energy \sqrt{s} far above the production threshold for top quarks and (2) we are not considering the transverse polarization for the top quarks. The contribution from C can be neglected since it is proportional to the electron mass.

The differential cross section at the one loop level is given by

$$\frac{d\sigma}{d\cos\theta} (\epsilon_L^- \epsilon_R^+ \rightarrow t_\uparrow \bar{t}_\uparrow) = \frac{d\sigma}{d\cos\theta} (\epsilon_L^- \epsilon_R^+ \rightarrow t_\downarrow \bar{t}_\downarrow) \\ = \left(\frac{3\pi\alpha^2}{2s} \beta \right) (A_{LR} \cos \xi - B_{LR} \sin \xi) \\ \times \left[(A_{LR} \cos \xi - B_{LR} \sin \xi)(1 + 2A + 2B) \right. \\ \left. - 2(\gamma^2 A_{LR} \cos \xi - \bar{B}_{LR} \sin \xi) B \right], \quad (7)$$

$$\frac{d\sigma}{d\cos\theta} (\epsilon_L^- \epsilon_R^+ \rightarrow t_\uparrow \bar{t}_\downarrow \text{ or } t_\downarrow \bar{t}_\uparrow) \\ = \left(\frac{3\pi\alpha^2}{2s} \beta \right) (A_{LR} \sin \xi + B_{LR} \cos \xi \pm D_{LR}) \\ \times \left[(A_{LR} \sin \xi + B_{LR} \cos \xi \pm D_{LR})(1 + 2A + 2B) \right. \\ \left. - 2(\gamma^2 A_{LR} \sin \xi + \bar{B}_{LR} \cos \xi \pm \bar{D}_{LR}) B \right]. \quad (8)$$

Here, the angle θ is the scattering angle of the top quark with respect to the electron in the zero momentum frame, α is the QED fine structure constant and $\gamma = 1/\sqrt{1-\beta^2}$.

The quantities $A_{LR}, B_{LR}, \bar{B}_{LR}, D_{LR}$ and \bar{D}_{LR} are defined by

$$\begin{aligned} A_{LR} &= [(f_{LL} + f_{LR})\sqrt{1-\beta^2} \sin \theta]/2, \\ B_{LR} &= [f_{LL}(\cos \theta + \beta) + f_{LR}(\cos \theta - \beta)]/2 = \bar{B}_{LR}(-\beta), \\ D_{LR} &= [f_{LL}(1 + \beta \cos \theta) + f_{LR}(1 - \beta \cos \theta)]/2 = \bar{D}_{LR}(-\beta), \end{aligned} \quad (9)$$

with

$$f_{IJ} = -Q_t + Q_e^I Q_t^J \frac{1}{\sin^2 \theta_W} \frac{s}{s - M_Z^2},$$

where M_Z is the Z mass (as mentioned before, we neglect the Z width) and $I, J \in (L, R)$. The electron couplings to the Z boson are

$$Q_e^L = \frac{2 \sin^2 \theta_W - 1}{2 \cos \theta_W}, \quad Q_e^R = \frac{\sin^2 \theta_W}{\cos \theta_W}.$$

The cross sections Eqs.(7,8) contain an infrared singularity (in the form factor A) that will be cancelled by the contributions from the real gluon emission. In the soft gluon approximation, it is very easy to calculate the real gluon contribution. As is well known, the amplitude for the soft gluon emissions can be written in the factorized form proportional to the tree amplitude. This means that the soft gluon emission does not change the spin configurations or momentum of the produced heavy quark pairs from the tree level values. Therefore the QCD radiative corrections enter mainly through the modifications of the vertex parts Eqs.(1,2). The cross section for the soft gluon emissions can be written as

$$\frac{d\sigma}{d \cos \theta} = J_{\text{IR}} \frac{d\sigma_0}{d \cos \theta}, \quad (10)$$

where the subscript 0 denotes the tree level cross section. The soft gluon contribution J_{IR} is defined by

$$J_{\text{IR}} \equiv -4\pi C_2(R) \alpha_s \int^{k^0=\omega_{\text{max}}} \frac{d^3 \vec{k}}{(2\pi)^3 2k^0} \left(\frac{t_\mu}{t \cdot k} - \frac{\bar{t}_\mu}{\bar{t} \cdot k} \right)^2,$$

where ω_{\max} is the cut-off of the soft gluon energy. This integral can be easily performed and we obtain

$$J_{\text{IR}} = 2\hat{\alpha}_s \left[\left(\frac{1+\beta^2}{\beta} \ln \frac{1+\beta}{1-\beta} - 2 \right) \ln \frac{4\omega_{\max}^2}{\lambda^2} + \frac{2}{\beta} \ln \frac{1+\beta}{1-\beta} - \frac{1+\beta^2}{\beta} \left[2\text{Li}_2 \left(\frac{2\beta}{1+\beta} \right) + \frac{1}{2} \ln^2 \frac{1+\beta}{1-\beta} \right] \right] .$$

By adding the one loop contributions Eqs.(7,8) and the soft gluon ones Eq.(10), one can see that the infrared singularities, $\ln \lambda$, are cancelled out and the finite results are obtained by replacing $2A$ by

$$\begin{aligned} & 2A + J_{\text{IR}} \\ &= 2\hat{\alpha}_s \left[\left(\frac{1+\beta^2}{\beta} \ln \frac{1+\beta}{1-\beta} - 2 \right) \ln \frac{4\omega_{\max}^2}{m^2} - 4 + \frac{2+3\beta^2}{\beta} \ln \frac{1+\beta}{1-\beta} + \frac{1+\beta^2}{\beta} \left\{ \ln \frac{1-\beta}{1+\beta} \left(3 \ln \frac{2\beta}{1+\beta} + \ln \frac{2\beta}{1-\beta} \right) + 4\text{Li}_2 \left(\frac{1-\beta}{1+\beta} \right) + \frac{1}{3}\pi^2 \right\} \right] , \end{aligned}$$

in Eqs.(7,8).

The cross sections for $\epsilon_{\bar{R}}\epsilon_L^\dagger$ can be obtained by interchanging L, R as well as \uparrow, \downarrow in the above formulae.

Since we are interested in maximizing the spin correlations of the top quark pairs we must vary the spin angle, ξ , to find the appropriate spin basis. At tree level, it is known that there exists the ‘‘off-diagonal’’ basis which makes the contributions from the like-spin configuration vanish [11]. At order $\mathcal{O}(\alpha_s)$, we find that definition of the off-diagonal basis for $\epsilon_{\bar{L}}\epsilon_R^\dagger$ scattering is not modified by QCD corrections, with the spin angle, ξ , satisfying the tree-level relationship

$$\tan \xi = \frac{A_{LR}}{B_{LR}} = \frac{(f_{LL} + f_{LR})\sqrt{1-\beta^2} \sin \theta}{f_{LL}(\cos \theta + \beta) + f_{LR}(\cos \theta - \beta)} . \quad (11)$$

The first order QCD corrected cross sections in this basis are

$$\frac{d\sigma}{d \cos \theta} \left(\epsilon_{\bar{L}}\epsilon_R^\dagger \rightarrow t_\uparrow\bar{t}_\uparrow \text{ and } t_\downarrow\bar{t}_\downarrow \right) = 0 , \quad (12)$$

$$\frac{d\sigma}{d\cos\theta} (\epsilon_L^- \epsilon_R^+ \rightarrow t_\uparrow \bar{t}_\downarrow \text{ or } t_\downarrow \bar{t}_\uparrow) = \left(\frac{3\pi\alpha^2}{2s} \beta \right) (\sqrt{A_{LR}^2 + B_{LR}^2} \mp D_{LR}) \quad (13)$$

$$\times \left[(\sqrt{A_{LR}^2 + B_{LR}^2} \mp D_{LR}) (1 + S_I) - 2 \left(\frac{\gamma^2 A_{LR}^2 + B_{LR} \bar{B}_{LR}}{\sqrt{A_{LR}^2 + B_{LR}^2}} \mp \bar{D}_{LR} \right) S_{II} \right],$$

where

$$S_I = 2A + J_{\text{IR}} + 2B \quad , \quad S_{II} = B \quad .$$

A similar result holds for $\epsilon_R^- \epsilon_L^+$ scattering.

In Fig.3 we show the differential cross sections in the off-diagonal basis, Eq.(11), for $\sqrt{s} = 400 \text{ GeV}$.

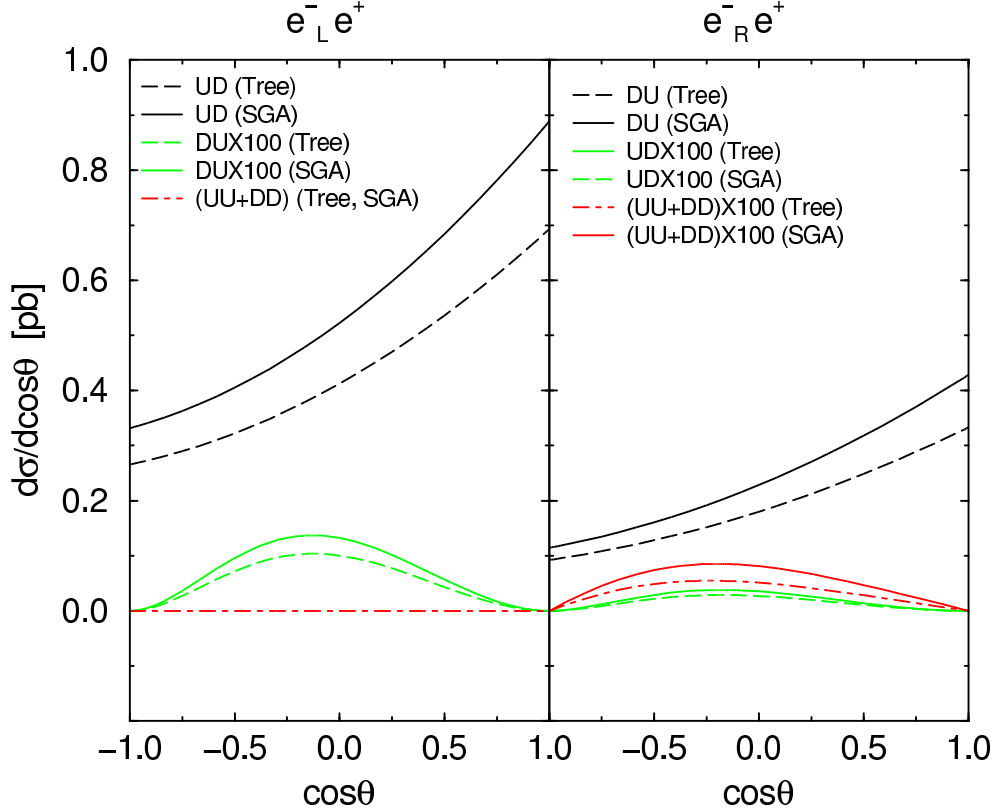


Figure 3: The cross sections in the off-diagonal basis, Eq.(11), at $\sqrt{s} = 400 \text{ GeV}$, $\omega_{\text{max}} = 10 \text{ GeV}$ for the $\epsilon^- \epsilon^+ \rightarrow t \bar{t}$ process: $t_\uparrow \bar{t}_\downarrow$ (UD), $t_\downarrow \bar{t}_\uparrow$ (DU) and $t_\uparrow \bar{t}_\uparrow + t_\downarrow \bar{t}_\downarrow$ (UU+DD). The suffix “Tree” and “SGA” mean the differential cross-section at the tree level and at the one-loop level in the soft gluon approximation. It should be noted that DU (UD) component for the $\epsilon_L^- \epsilon^+$ ($\epsilon_R^- \epsilon^+$) process is multiplied by 100.

The following values for the parameters of the standard model were used

$$m \equiv M_{\text{top}} = 175 \text{ GeV} \quad , \quad M_Z = 91.187 \text{ GeV} \quad ,$$

$$\alpha = \frac{1}{128} \quad , \quad \alpha_s(M_Z^2) = 0.118 \quad , \quad \sin^2 \theta_W = 0.2315 \quad .$$

We use \sqrt{s} as the renormalization scale and the pole mass for the top quark. For $\epsilon_L^- \epsilon_R^+$ scattering the up-up ($t_\uparrow \bar{t}_\uparrow$) and the down-down $t_\downarrow \bar{t}_\downarrow$ components are identically zero. The total cross section is more than 99% up-down $t_\uparrow \bar{t}_\downarrow$ and less than 1% down-up $t_\downarrow \bar{t}_\uparrow$. For $\epsilon_R^- \epsilon_L^+$ scattering the up-up ($t_\uparrow \bar{t}_\uparrow$) and the down-down $t_\downarrow \bar{t}_\downarrow$ components are non-zero because we have used the off-diagonal basis for $\epsilon_L^- \epsilon_R^+$ scattering. However the down-up $t_\downarrow \bar{t}_\uparrow$ component is still more than 99% of the total cross section.

Although there exist a magnetic moment modification to the $\gamma/Z - t - \bar{t}$ vertex from QCD corrections, this does not change the behavior of the spin dependent cross sections in the off-diagonal basis. The QCD corrections, however, make the differential cross sections larger by $\sim 30\%$ compared to the tree level ones at this \sqrt{s} . Thus the off-diagonal basis continues to display very strong spin correlations for the top quark pairs even after taking the QCD corrections into account, at least in the soft gluon approximation.

In the previous paragraph the cut-off energy for the soft gluon has been chosen as $\omega_{\text{max}} = 10 \text{ GeV}$. The results, of course, depend on the value of ω_{max} . The ω_{max} dependence of the cross section is examined in Fig.4. The cross section behaves quite uniformly as the value of ω_{max} is changed thus the above conclusions remain qualitatively the same for any reasonable value of ω_{max} .

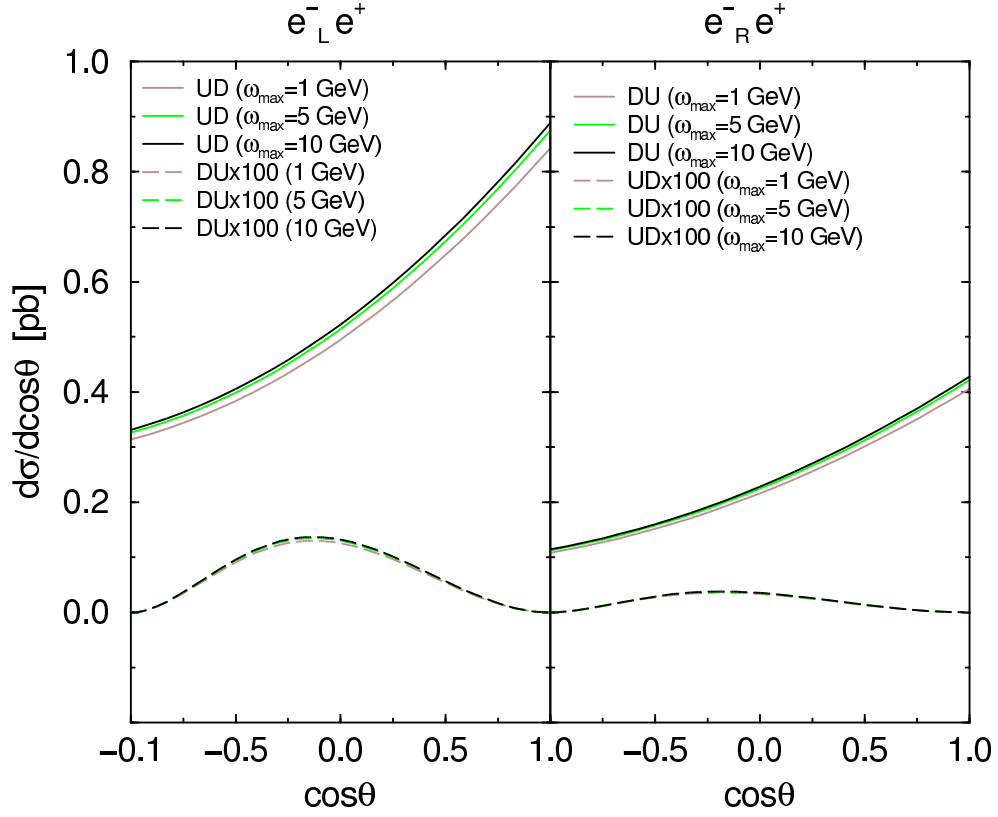


Figure 4: The ω_{\max} dependence of the cross-sections in the off-diagonal basis at $\sqrt{s} = 400$ GeV. The DU (UD) component for the $e_L^- e^+$ ($e_R^- e^+$) process is multiplied by 100.

3 Single Spin Correlations in e^+e^- Process

The soft gluon approximation used in the last section has two shortcomings. First, soft gluon emission cannot change the spin of the heavy quarks and second the heavy quark pairs are always back to back. Neither of these approximations is valid for hard gluon emission. Hence it is possible that the full $\mathcal{O}(\alpha_s)$ QCD corrections might completely change the conclusions of the previous section. Therefore, in this section, we investigate the full $\mathcal{O}(\alpha_s)$ QCD corrections. Since, in the presence of a hard gluon, the top and anti-top quarks are not generally produced back-to-back, it is more sensible to consider the single heavy quark spin correlations, namely the inclusive cross section for the production of the top (or anti-top) quark in a particular spin configuration. We have organized this section as follows. After defining the kinematics and our conventions, we give the polarized cross section for the top quark using a generic spin basis closely related to the spin basis of the previous section. The numerical analysis will be relegated to the next section.

3.1 Amplitudes and Kinematics

The principle result of this section will be the inclusive cross section for polarized top quark production, $e^+e^- \rightarrow t_\uparrow \text{ or } t_\downarrow + X$, where $X = \bar{l} \text{ or } \bar{l}g$. (The cross section for the anti-top quark inclusive production can be easily obtained from the results in this section.) Since the vertex corrections are the same as in the previous section all that is required is the full real gluon emission contributions. The real gluon emission diagrams to leading order in α_s are given in Fig.5.

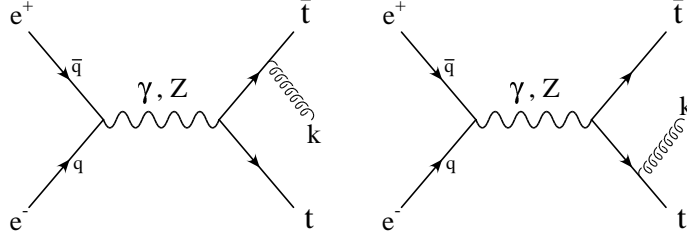


Figure 5: The real gluon emission contributions to top quark pair production.

This figure also defines the momenta of particles. We will use the spinor helicity method for massive fermions [10] to calculate the squares of these amplitudes for a polarized top quark. The top quark momentum t is decomposed into a sum of two massless momenta t_1, t_2 such that in the rest frame of the top quark the spatial momentum of t_1 defines the spin axis for the top quark.

$$t = t_1 + t_2 \quad , \quad m s_t = t_1 - t_2 \quad ,$$

where s_t is the spin four vector of the top quark.

The amplitude for Fig.5 is given by

$$\begin{aligned}
M(\epsilon_L^- \epsilon_R^+ \rightarrow t_\alpha \bar{t}_\beta g) &= \bar{v}_+(\bar{q}) \gamma_L^\mu u_\downarrow(q) \\
&\times \bar{u}_\alpha(t) \left[\frac{1}{2\bar{t} \cdot k} \left(\frac{a_{LL}}{2} \gamma_L^\mu + \frac{a_{LR}}{2} \gamma_R^\mu \right) (-\not{\bar{t}} - \not{k} + m) \gamma_\nu \right. \\
&\quad \left. + \frac{1}{2t \cdot k} \gamma_\nu (\not{t} + \not{k} + m) \left(\frac{a_{LL}}{2} \gamma_L^\mu + \frac{a_{LR}}{2} \gamma_R^\mu \right) \right] T^a v_\beta(\bar{t}) \epsilon_a^\nu(k) \quad ,
\end{aligned} \tag{14}$$

where α, β are the spin indices for quarks and ϵ is the polarization vector of the gluon. T^a is the color matrix. The coupling constants a_{LI} are defined as follows:

$$\frac{a_{LI}}{2} = \frac{e^2 g}{s} f_{LI} \quad .$$

The expressions for the squares of the amplitudes given below have been summed over the spins of the unobserved particles (the anti-top quark and gluon) as well as the

colors of the final state particles. Let us write the square of the amplitude for the top quark with spin “up” as

$$\begin{aligned}
& |M(\epsilon_L^- \epsilon_R^+ \rightarrow t \bar{t} g)|^2 \\
&= N_c C_2(R) \left[\frac{1}{(\bar{t} \cdot k)^2} T_1 + \frac{1}{(\bar{t} \cdot k)(t \cdot k)} T_2 + \frac{1}{(t \cdot k)^2} T_3 \right]. \quad (15)
\end{aligned}$$

After some calculation, we find

$$\begin{aligned}
T_1 &= 4 |a_{LL}|^2 [(\bar{t} \cdot k)(q \cdot k) - m^2 q \cdot (\bar{t} + k)] (t_2 \cdot \bar{q}) \\
&+ 4 |a_{LR}|^2 [(\bar{t} \cdot k)(\bar{q} \cdot k) - m^2 \bar{q} \cdot (\bar{t} + k)] (t_1 \cdot q) \\
&- [a_{LL} a_{LR}^* ((\bar{t} \cdot k) + m^2) \text{Tr}(\omega_+ t_1 t_2 \bar{q} q) + c.c.] , \\
T_2 &= |a_{LL}|^2 [4(t \cdot \bar{t})(\bar{t} \cdot q)(t_2 \cdot \bar{q}) + (t_2 \cdot \bar{q}) \text{Tr}(\omega_+ q k t \bar{t}) + (\bar{t} \cdot q) \text{Tr}(\omega_- t_2 \bar{q} k \bar{t})] \\
&+ |a_{LR}|^2 [4(t \cdot \bar{t})(\bar{t} \cdot \bar{q})(t_1 \cdot q) + (t_1 \cdot q) \text{Tr}(\omega_- \bar{q} k t \bar{t}) + (\bar{t} \cdot \bar{q}) \text{Tr}(\omega_+ t_1 q k \bar{t})] \\
&+ a_{LL} a_{LR}^* [(t \cdot \bar{t}) \text{Tr}(\omega_+ t_1 t_2 \bar{q} q) - (k \cdot q) \text{Tr}(\omega_+ t_1 t_2 \bar{q} k) \\
&\quad + \frac{1}{2} \text{Tr}(\omega_+ t_2 t_1 q k t \bar{q}) + \frac{1}{2} \text{Tr}(\omega_+ t_1 t_2 \bar{q} q k \bar{t})] \\
&+ a_{LL}^* a_{LR} [(t \cdot \bar{t}) \text{Tr}(\omega_- t_2 t_1 q \bar{q}) - (k \cdot \bar{q}) \text{Tr}(\omega_- t_2 t_1 q k) \\
&\quad + \frac{1}{2} \text{Tr}(\omega_- t_1 t_2 \bar{q} k t q) + \frac{1}{2} \text{Tr}(\omega_- t_2 t_1 q \bar{q} k \bar{t})] \\
&+ c.c. \\
T_3 &= 2 |a_{LL}|^2 [-m^2(k \cdot \bar{q}) - 2(m^2 + (t \cdot k))(t_2 \cdot \bar{q}) + 2((t + k) \cdot \bar{q})(t_2 \cdot k)] (\bar{t} \cdot q) \\
&+ 2 |a_{LR}|^2 [-m^2(k \cdot q) - 2(m^2 + (t \cdot k))(t_1 \cdot q) + 2((t + k) \cdot q)(t_1 \cdot k)] (\bar{t} \cdot \bar{q}) \\
&- \frac{m^2}{2} [a_{LL} a_{LR}^* \{2 \text{Tr}(\omega_+ t_1 t_2 \bar{q} q) + \text{Tr}(\omega_+ k t_2 \bar{q} q) + \text{Tr}(\omega_+ t_1 k \bar{q} q)\} + c.c.] ,
\end{aligned}$$

where $\omega_{\pm} \equiv \frac{1 \pm \gamma_5}{2}$ and that all momentum, p , under the “Tr” operator are understood to be \not{p} . By interchanging the t_1 and t_2 vectors in the above expressions, we can get the amplitude square for the top quark with spin “down”. Since we neglect the Z width in this paper, all the coupling constants a_{LI} are real.

To define the spin basis for the top quark we naturally extend the spin definition of the previous section to the present case. The top quark spin is decomposed along the

direction \mathbf{s}_t in the rest frame of the top quark which makes an angle ξ with the sum of the anti-top quark and the gluon momenta in the clockwise direction, see Fig.6.

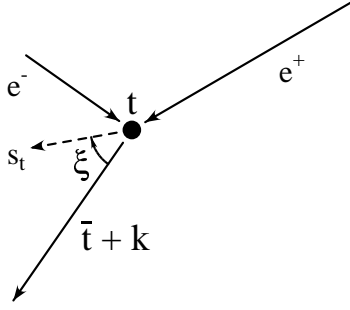


Figure 6: The spin basis for the top quark in the process $e^- e^+ \rightarrow t \bar{l} g$.

To calculate the cross section from Eq.(15), we take the CM frame in which the $e^+ e^-$ beam line coincides with the z -axis,

$$q = \frac{\sqrt{s}}{2}(1, 0, 0, 1) \quad , \quad \bar{q} = \frac{\sqrt{s}}{2}(1, 0, 0, -1) .$$

We specify the variables x, y and z which are related to CM energies of the gluon, top and anti-top quarks by

$$x \equiv 1 - \frac{2k \cdot (q + \bar{q})}{s} \quad , \quad y \equiv 1 - \frac{2t \cdot (q + \bar{q})}{s} \quad , \quad z \equiv 1 - \frac{2\bar{t} \cdot (q + \bar{q})}{s} .$$

The momenta of the final state particles, in terms of these variables, are

$$k = \frac{\sqrt{s}}{2}(1 - x, (1 - x)\hat{k}) \quad , \quad t = \frac{\sqrt{s}}{2}(1 - y, a(y)\hat{t}) \quad , \quad \bar{t} = \frac{\sqrt{s}}{2}(1 - z, a(z)\hat{\bar{t}}) \quad ,$$

where $\hat{}$ means the unit space vector and

$$a(y) \equiv \sqrt{(1 - y)^2 - a} \quad , \quad a(z) \equiv \sqrt{(1 - z)^2 - a} \quad ,$$

with $a \equiv 4m^2/s$. Fig.7 defines the orientation of the top and anti-top momenta and by energy-momentum conservation the momentum of the gluon is also determined.

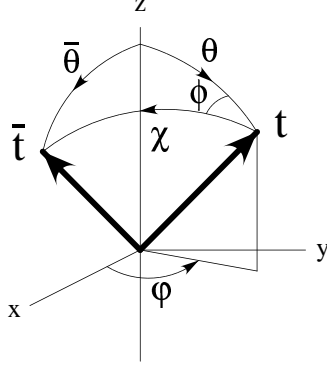


Figure 7: The momentum (unit vectors) configuration of the top and anti-top quarks in the CM frame. The momentum of e^- (e^+) is in the $+z$ ($-z$) direction.

One can easily obtain the spin four vector of the top quark in the CM frame by boosting the spin vector characterized by ξ in the top quark rest frame in the direction of top quark momentum by $\beta(y)$ (the speed of the top quark in the CM frame). The explicit form for t_1 ($t_2 = t - t_1$) is given by

$$\begin{aligned}
t_1^0 &= \frac{m}{2} [\gamma(y) (1 - \beta(y) \cos \xi)] , \\
t_1^1 &= \frac{m}{2} [\gamma(y) (\beta(y) - \cos \xi) \sin \theta \cos \varphi + \sin \xi \cos \theta \cos \varphi] , \\
t_1^2 &= \frac{m}{2} [\gamma(y) (\beta(y) - \cos \xi) \sin \theta \sin \varphi + \sin \xi \cos \theta \sin \varphi] , \\
t_1^3 &= \frac{m}{2} [\gamma(y) (\beta(y) - \cos \xi) \cos \theta - \sin \xi \sin \theta] ,
\end{aligned} \tag{16}$$

where

$$\sqrt{a} \gamma(y) = 1 - y \quad , \quad \sqrt{a} \gamma(y) \beta(y) = a(y) .$$

If we eliminate the gluon momentum k using the energy momentum conservation and use the angular variables χ, ϕ in Fig.7 to specify the orientation of the anti-top quark (if one eliminates the anti-top momentum, one can proceed in the similar way by introducing other angular variables), the square of the amplitude Eq.(15) can be

written as

$$|M(\epsilon_L^- \epsilon_R^+ \rightarrow t \bar{t} g)|^2 = \frac{s}{8} N_c C_2(R) \left[a_{LL}^2 M_1 + a_{LR}^2 M_2 + a_{LL} a_{LR} M_3 \right], \quad (17)$$

where M_i are the functions of y, z , angles defined above and the spin orientation ξ .

$$\begin{aligned} M_1 &= \frac{2}{yz} \left[(1-y)^2 + a^2(y) \cos^2 \theta + (1-z)^2 + a^2(z) \cos^2 \bar{\theta} \right] \\ &- a \left(\frac{1}{yz} + \frac{1}{y^2} \right) (1-y^2 + a^2(y) \cos^2 \theta) - a \left(\frac{1}{yz} + \frac{1}{z^2} \right) (1-z^2 + a^2(z) \cos^2 \bar{\theta}) \\ &+ 2 \left(\frac{2-2y-a}{yz} - \frac{a}{y^2} \right) a(y) \cos \theta - 2 \left(\frac{2-2z-a}{yz} - \frac{a}{z^2} \right) a(z) \cos \bar{\theta} \\ &+ \frac{1}{yz^2} (1-z-a(z) \cos \bar{\theta}) \left[y(1-a(z) \cos \bar{\theta}) - z(1-a(y) \cos \theta) \right] (\delta t \cdot \bar{t}) \\ &- \frac{1}{yz^2} (1-z-a(z) \cos \bar{\theta}) \left[y-z+(y+z)(z-a(z) \cos \bar{\theta}) \right] (\delta t \cdot (\bar{q}+q)) \\ &+ \frac{a}{yz} \left(\frac{1}{y} + \frac{1}{z} \right) \left[y(1-a(z) \cos \bar{\theta}) + z(1+a(y) \cos \theta) \right] (\delta t \cdot \bar{q}) \\ &- \frac{2}{yz} \left[(1-y+a(y) \cos \theta) + (1-y-z)(1-z-a(z) \cos \bar{\theta}) \right] (\delta t \cdot \bar{q}), \\ M_2 &= M_1(\cos \theta \rightarrow -\cos \theta, \cos \bar{\theta} \rightarrow -\cos \bar{\theta}, \delta t \rightarrow -\delta t) \\ M_3 &= 2a \left\{ \frac{4}{yz} - \frac{4}{y} - \frac{4}{z} - \frac{(y+z)^2}{yz} + \frac{(y+z)^2}{yz} \cos^2 \theta_k \right\} - 2a^2 \left(\frac{1}{y} + \frac{1}{z} \right)^2 \\ &+ \frac{a}{yz} \left(\frac{1}{y} + \frac{1}{z} \right) (ya(z) \cos \bar{\theta} - za(y) \cos \theta) (\delta t \cdot (\bar{q}+q)) \\ &- \frac{2}{yz} \left[a(y) \cos \theta + (1-y-z)a(z) \cos \bar{\theta} \right] (\delta t \cdot (\bar{q}+q)) \\ &+ a \left(\frac{1}{y} + \frac{1}{z} \right)^2 (\delta t \cdot (\bar{q}-q)) + \frac{2}{yz} [z(y+z) - 2(1-y-z)] (\delta t \cdot (\bar{q}-q)) \\ &+ \frac{2}{yz} \left[(1-y)a(z) \cos \bar{\theta} + (3+z)a(y) \cos \theta \right] (\delta t \cdot \bar{t}). \end{aligned}$$

In the above equations, θ_k is the angle between the z axis and the gluon momentum

$$(y+z) \cos \theta_k = -a(y) \cos \theta - a(z) \cos \bar{\theta},$$

and δt is defined as

$$\delta t \equiv \frac{4}{s} (t_1 - t_2).$$

Using Eq.(16) we find that the products of δt with momenta q , \bar{q} and \bar{l} are

$$\begin{aligned}\delta t \cdot q &= \{(1-y)\cos\theta - a(y)\}\cos\xi + \sqrt{a}\sin\theta\sin\xi, \\ \delta t \cdot \bar{q} &= \{-(1-y)\cos\theta - a(y)\}\cos\xi - \sqrt{a}\sin\theta\sin\xi, \\ \delta t \cdot \bar{l} &= \{-(1-z)a(y) + (1-y)a(z)\cos\chi\}\cos\xi \\ &\quad + \sqrt{a}a(z)\sin\xi\sin\chi\cos\phi.\end{aligned}$$

The unpolarized top quark production process is given by dropping the spin dependent parts (terms proportional to δt) in Eq.(17). As a check we have reproduced the results of Ref. [12] by putting $a_{LL} = a_{LR} = -\frac{2e^2g}{s}Q_q$.

The cross section is given by

$$d\sigma(\epsilon_L^-\epsilon_R^+ \rightarrow t\bar{l}g) = \frac{1}{2s}|M(\epsilon_L^-\epsilon_R^+ \rightarrow t\bar{l}g)|^2(PS)_3, \quad (18)$$

where $(PS)_3$ is the three particle phase space.

$$(PS)_3 = \frac{d^3t}{(2\pi)^3 2t^0} \frac{d^3\bar{l}}{(2\pi)^3 2\bar{l}^0} \frac{d^3k}{(2\pi)^3 2k^0} (2\pi)^4 \delta^4(t + \bar{l} + k - q - \bar{q}).$$

We introduce a small mass λ for the gluon to regularize the infrared singularities. It is easy to rewrite the above phase space integral as,

$$\begin{aligned}\int (PS)_3 &= \frac{s}{(4\pi)^5} \int_{y_-}^{y_+} dy \int_{z_-(y)}^{z_+(y)} dz \\ &\quad \times \int d\Omega d\cos\chi d\phi \delta\left(\cos\chi - \frac{y+z+yz+a-1-2a_\lambda}{a(y)a(z)}\right),\end{aligned}$$

where $d\Omega = d\cos\theta d\varphi$ is the solid angle for the top quark and $a_\lambda \equiv \lambda^2/s$. The integration regions over y and z are determined by the condition $|\cos\chi| \leq 1$,

$$\begin{aligned}y_+ &= 1 - \sqrt{a} \quad , \quad y_- = \sqrt{aa_\lambda} + a_\lambda, \\ z_\pm(y) &= \frac{2}{4y+a} \left[y \left(1 - y - \frac{a}{2} + a_\lambda \right) + a_\lambda \pm a(y) \sqrt{(y-a_\lambda)^2 - aa_\lambda} \right].\end{aligned}$$

The integration over the angle ϕ is not difficult if one uses the relation

$$\cos\bar{\theta} = \cos\theta\cos\chi + \sin\theta\sin\chi\cos\phi.$$

The integrals we need are the following:

$$\begin{aligned}
\int \cos \bar{\theta} d\phi &= 2\pi \cos \theta \cos \chi , \\
\int \cos^2 \bar{\theta} d\phi &= 2\pi \left[\cos^2 \theta + \frac{1}{2}(1 - 3 \cos^2 \theta) \sin^2 \chi \right] , \\
\int \cos^2 \theta_k d\phi &= 2\pi \left[\cos^2 \theta + \frac{1}{2}(1 - 3 \cos^2 \theta) \frac{a^2(z)}{(y+z)^2} \sin^2 \chi \right] , \\
\int \cos \bar{\theta} \cos \phi d\phi &= \pi \sin \theta \sin \chi , \\
\int \cos^2 \bar{\theta} \cos \phi d\phi &= 2\pi \sin \theta \cos \theta \sin \chi \cos \chi .
\end{aligned}$$

Due to the δ function in the phase space integral, the angle χ is a function of y and z :

$$\begin{aligned}
\cos \chi &= \frac{y+z+yz+a-1}{a(y)a(z)} , \\
\sin^2 \chi &= \frac{4yz(1-z-y) - a(y+z)^2}{a^2(y)a^2(z)} ,
\end{aligned}$$

where we have put a_λ to be zero since the $\lambda \rightarrow 0$ limit does not produce any singularities in the (squared) amplitude. The remaining integrals to get the cross section are over the variables y and z . According to the type of integrand, we group the phase space integrals (after the integrations over the angular variables) into four distinct classes $\{J_i\}$, $\{N_i\}$, $\{L_i\}$ and $\{K_i\}$ [15]. The individual integrals of these classes are summarized in Appendix A.

3.2 Cross Section in the Generic Spin Basis

We write the inclusive cross section for the top quark in the following form.

$$\frac{d\sigma}{d\cos\theta}(\bar{e}_L e_R^+ \rightarrow t_\uparrow X) = \frac{3\pi\alpha^2}{4s} \sum_{klmn} (D_{klmn} + \hat{\alpha}_s C_{klmn}) \cos^k \theta \sin^l \theta \cos^m \xi \sin^n \xi , \quad (19)$$

where D_{klmn} are the contributions from the tree and the one-loop diagrams and C_{klmn} are from the real emission diagrams. Let us first write down the D_{klmn} ,

$$D_{0000} = \beta[f_{LL}^2 + f_{LR}^2 + 2af_{LL}f_{LR}](1 + \hat{\alpha}_s V_I)$$

$$\begin{aligned}
& -\beta[2(f_{LL} + f_{LR})^2 - \beta^2(f_{LL} - f_{LR})^2]\hat{\alpha}_s V_{II} , \\
D_{2000} &= \beta^3(f_{LL}^2 + f_{LR}^2)(1 + \hat{\alpha}_s V_I) + \beta^3(f_{LL} - f_{LR})^2 \hat{\alpha}_s V_{II} , \\
D_{1000} &= 2\beta^2(f_{LL}^2 - f_{LR}^2)(1 + \hat{\alpha}_s V_I) , \\
D_{0010} &= \beta^2(f_{LL}^2 - f_{LR}^2)(1 + \hat{\alpha}_s V_I) , \\
D_{2010} &= \beta^2(f_{LL}^2 - f_{LR}^2)(1 + \hat{\alpha}_s V_I) , \\
D_{1010} &= \beta[(f_{LL} + f_{LR})^2 + \beta^2(f_{LL} - f_{LR})^2](1 + \hat{\alpha}_s V_I) \\
& \quad - 2\beta[(f_{LL} + f_{LR})^2 - \beta^2(f_{LL} - f_{LR})^2]\hat{\alpha}_s V_{II} , \\
D_{0101} &= \frac{\beta}{\sqrt{a}}(f_{LL} + f_{LR})^2[a(1 + \hat{\alpha}_s V_I) - (1 + a)\hat{\alpha}_s V_{II}] , \\
D_{1101} &= \frac{\beta^2}{\sqrt{a}}(f_{LL}^2 - f_{LR}^2)[a(1 + \hat{\alpha}_s V_I) - (1 - a)\hat{\alpha}_s V_{II}] ,
\end{aligned}$$

with

$$\beta = \beta(0) = \sqrt{1 - a} \quad ; \quad \hat{\alpha}_s V_I = 2A + 2B \quad ; \quad \hat{\alpha}_s V_{II} = B .$$

A, B are defined in Eqs.(4,5).

For the C_{klmn} we find,

$$\begin{aligned}
C_{0000} &= 2(f_{LL}^2 + f_{LR}^2) \left[J_{\text{IR}}^1 - (4 - a)J_3 + (2 + a)J_2 + aJ_1 + \frac{1}{4}R_1 \right] \\
& \quad + 4a f_{LL} f_{LR} \left[J_{\text{IR}}^1 - 4J_3 - J_2 - J_1 + \frac{1}{4}R_2 \right] , \\
C_{2000} &= 2(f_{LL}^2 + f_{LR}^2) \left[(1 - a)J_{\text{IR}}^1 - (4 - a)J_3 + (2 - a)J_2 - aJ_1 - \frac{3}{4}R_1 \right] \\
& \quad + 4a f_{LL} f_{LR} \left[J_2 + J_1 - \frac{3}{4}R_2 \right] , \\
C_{1000} &= 2(f_{LL}^2 - f_{LR}^2) \left[(1 - a)J_{\text{IR}}^2 + aN_{10} - 2(4 - 3a)N_9 \right. \\
& \quad \left. - (4 - 5a)N_8 - 2N_7 + 2N_6 + 6N_3 + 2N_2 \right] , \\
C_{0010} &= \frac{1}{2} C_{1000} \\
& \quad + (f_{LL}^2 - f_{LR}^2) \left[-4N_6 - aN_4 - aN_3 - aN_2 + (4 - a)N_1 + \frac{1}{2}R_3 \right] , \\
C_{2010} &= C_{0010} - 2(f_{LL}^2 - f_{LR}^2)R_3 , \\
C_{1010} &= (f_{LL}^2 + f_{LR}^2) \left[2(2 - a)J_{\text{IR}}^1 + 2aJ_4 - 2(8 - 5a)J_3 \right.
\end{aligned}$$

$$\begin{aligned}
& - 2a(1-a)L_8 - 2a(1-a)L_7 - 2(4+3a)L_6 + 2(4-3a)L_5 \\
& + 2aL_4 + a(10-a)L_3 + (8-6a-a^2)L_2 - 2(4-3a+a^2)L_1 \Big] \\
& + 2a f_{LL}f_{LR} \left[2J_{\text{IR}}^1 - 8J_3 + 4L_6 + 4L_5 + aL_3 + aL_2 - 2(2-a)L_1 \right] , \\
C_{0101} = & \frac{\sqrt{a}}{2} (f_{LL}^2 + f_{LR}^2) \left[4J_{\text{IR}}^1 - (8+a)J_3 - (8-a)(1-a)L_7 - (12+a)L_6 \right. \\
& \left. - 2aL_5 + 2aL_4 + (8+a)L_3 + (4-5a)L_2 + 4(2-a)L_1 \right] \\
& + \sqrt{a} f_{LL}f_{LR} \left[4J_{\text{IR}}^1 - (16-a)J_3 - a(1-a)L_7 + (4+a)L_6 \right. \\
& \left. + 2aL_5 + aL_3 - (4-3a)L_2 + 2aL_1 \right] , \\
C_{1101} = & \frac{\sqrt{a}}{2} C_{1000} + \sqrt{a} (f_{LL}^2 - f_{LR}^2) \\
& \times \left[-aN_{10} - 9aN_9 + 2N_7 - 2N_6 - \frac{1}{2}(12+a)N_3 + \frac{a}{2}N_2 - (12+a)N_1 \right. \\
& \left. - a(1+a)K_8 + a(1-a)K_7 + 9a(1-a)K_6 - 3a(5+a)K_5 \right. \\
& \left. - (12+a)K_4 + (4-5a)K_3 - 3(4+5a)K_2 + 3(4+a)(1-a)K_1 \right] ,
\end{aligned}$$

where we have defined

$$\begin{aligned}
J_{\text{IR}}^1 &= (2-a)J_6 - aJ_5 , \\
J_{\text{IR}}^2 &= 2(2-a)N_{13} - aN_{12} - aN_{11} , \\
R_1 &= -4a(1-a)L_7 - 4(2-a)L_6 - 8(1-a)L_5 \\
&+ a^2L_4 + a(2+3a)L_3 - a(2-a)L_2 + (8-8a+3a^2)L_1 , \\
R_2 &= -4L_6 - 4L_5 - aL_3 - aL_2 + 2(2-a)L_1 , \\
R_3 &= a^2N_{10} + 3a(2+a)N_9 + 4aN_3 - 2aN_2 + 8(1+a)N_1 \\
&+ 2a^2K_8 - a^2(1-a)K_7 - 3a(1-a)(2+a)K_6 + 6a(1+2a)K_5 \\
&+ 2(4+3a)K_4 + (a^2+6a-8)K_3 + 3a(8+a)K_2 - 12a(1-a)K_1 .
\end{aligned}$$

Note that the integrals J_{IR}^1 , J_{IR}^2 namely J_5 , J_6 , N_{11} , N_{12} and N_{13} contain the infrared singularity. This singularity is exactly cancelled out in the sum Eq.(19) by the contributions from D_{klmn} . We are now ready to discuss our numerical results.

4 Numerical Results

We are now in the position to give the cross section for polarized top quark production for any e^+e^- collider. Since we did not specify the spin angle ξ for the top quark, we can predict the polarized cross section for any top quark spin. The spin configurations we will display are the helicity, the beamline and the off-diagonal bases for centre of mass energies $\sqrt{s} = 400 \text{ GeV}, 800 \text{ GeV}, 1500 \text{ GeV}$.

Table 1 contains the values of the maximum centre of mass speed, the running α_s , the Born cross section, the next to leading order cross section and the fractional $\mathcal{O}(\alpha_s)$ enhancement of the Born cross section (κ) for top quark pair production in $e_L^-e^+$ scattering.

\sqrt{s}	400 GeV	800 GeV	1500 GeV
β	0.484	0.899	0.972
$\alpha_s(s)$	0.0980	0.0910	0.0854
$\sigma_{Total} \text{ Tree (pb)}$	0.8707	0.3531	0.1047
$\sigma_{Total} \mathcal{O}(\alpha_s) \text{ (pb)}$	1.113	0.3734	0.1084
κ	0.2783	0.05749	0.03534

Table 1: The values of β , α_s , Born and next to leading order cross sections and κ for $e_L^-e^+$ scattering.

At $\sqrt{s} = 400 \text{ GeV}$ the QCD corrections enhance the total cross section by $\sim 30\%$ compared to the Born results whereas at higher energies, 800 and 1500 GeV, the enhancements are at the $\sim 5\%$ level.

First we will show the numerical values for the coefficients ($D_{klmn} + \hat{\alpha}_s C_{klmn}$) in Eq.(19). Since the dominant effect of the $\mathcal{O}(\alpha_s)$ corrections is a multiplicative enhancement of the tree level result we have chosen to write

$$D_{klmn} + \hat{\alpha}_s C_{klmn} \equiv (1 + \kappa) D_{klmn}^0 + S_{klmn}.$$

The $(1 + \kappa) D_{klmn}^0$ terms are the multiplicative enhancement of the tree level result

whereas the S_{klmn} give the α_s deviations to the spin correlations. The numerical value of these coefficients are given in Table 2.

	400 GeV	800 GeV	1500 GeV
$(1 + \kappa)D_{0000}^0$	1.511	1.722	1.671
$(1 + \kappa)D_{2000}^0$	0.2404	1.241	1.526
$(1 + \kappa)D_{1000}^0$	0.7809	2.126	2.406
$(1 + \kappa)D_{0010}^0$	0.3905	1.063	1.203
$(1 + \kappa)D_{2010}^0$	0.3905	1.063	1.203
$(1 + \kappa)D_{1010}^0$	1.751	2.963	3.197
$(1 + \kappa)D_{0101}^0$	1.452	1.100	0.6186
$(1 + \kappa)D_{1101}^0$	0.3416	0.4650	0.2807
S_{0000}	-0.002552	0.0005645	0.01172
S_{2000}	0.007655	-0.001682	-0.03516
S_{1000}	0.02154	0.01224	-0.02085
S_{0010}	0.01094	0.01586	0.008357
S_{2010}	0.01059	-0.006158	-0.03614
S_{1010}	0.004433	-0.02030	-0.06134
S_{0101}	-0.006564	-0.04413	-0.04952
S_{1101}	0.007920	-0.01270	-0.02047

Table 2: The values of $(1 + \kappa)D_{klmn}^0$ and S_{klmn} for $\epsilon_L^- \epsilon^+$ scattering.

The ratios $S_{klmn}/(1 + \kappa)D_{klmn}^0$ are never larger than 10% and are typically of order a few percent. Hence the $\mathcal{O}(\alpha_s)$ corrections make only small changes to the spin orientation of the top quark.

To illustrate the different spin bases we present the top quark production cross section in the three different spin bases discussed in ref. [11]. One is the usual helicity basis which corresponds to $\cos \xi = +1$. The second is the beamline basis in which the top quark spin is aligned with the positron in the top quark rest frame (ξ for the beamline basis is obtained from Eq.(11) with $f_{LR} = 0$). The third corresponds to the off-diagonal basis which has been defined in Eq.(11). Note that as $\beta \rightarrow 1$, all of these bases coincide. Therefore, at an extremely high energy collider, there will be no significant difference between these bases.

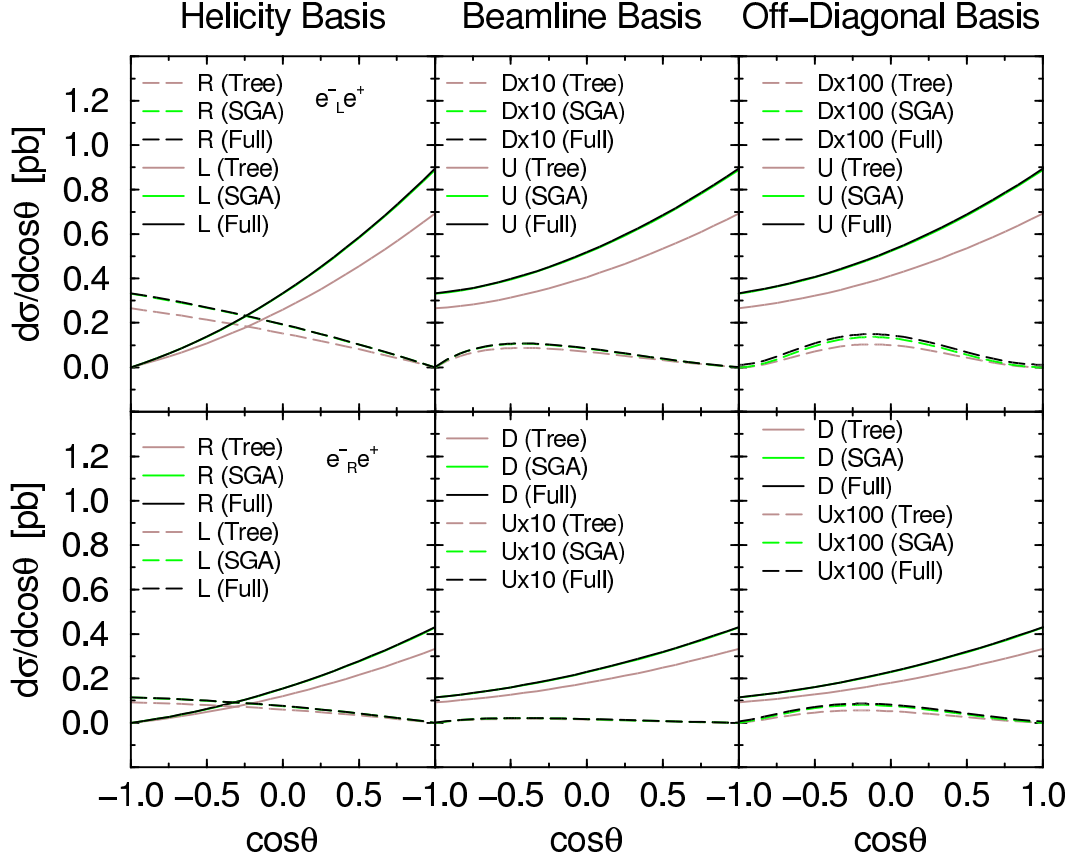


Figure 8: The cross sections in the helicity, beamline and off-diagonal bases at $\sqrt{s} = 400$ GeV. Here we use a “beamline basis”, in which the top quark axis is the positron direction in the top rest frame, for each $e^-_L e^+$ and $e^-_R e^+$ scattering.

In Fig. 8 we give the results for $\sqrt{s} = 400$ GeV for both $e^-_L e^+$ and $e^-_R e^+$ scattering using the helicity, beamline and off-diagonal spin bases. This figure shows the Born, SGA and the full QCD results for all three spin bases. Since the SGA results almost coincide with the full QCD results the probability that hard gluon emission flips the spin of the top quark is very small. Clearly, the qualitative features of the cross sections remain the same as those in the leading order analysis. That is the top quarks are produced with very high polarization in polarized $e^+ e^-$ scattering. In Table 3 we give

the fraction of the top quarks in the dominant spin configuration for $e_L^- e^+$ scattering,

$$\sigma\left(\epsilon_L^- e^+ \rightarrow t \uparrow X(\bar{l} \text{ or } \bar{l}g)\right) / \sigma_L^{Total}$$

for the three bases. Similar results also hold for $e_R^- e^+$ scattering.

$\sqrt{s} = 400 \text{ GeV}$	Helicity	Beamline	Off-Diagonal
Tree	0.6636	0.9881	0.9988
$\mathcal{O}(\alpha_s)$	0.6681	0.9885	0.9985

Table 3: The fraction of the $e_L^- e^+$ cross section in the dominant spin at $\sqrt{s} = 400 \text{ GeV}$ for the helicity, beamline and off-diagonal bases.

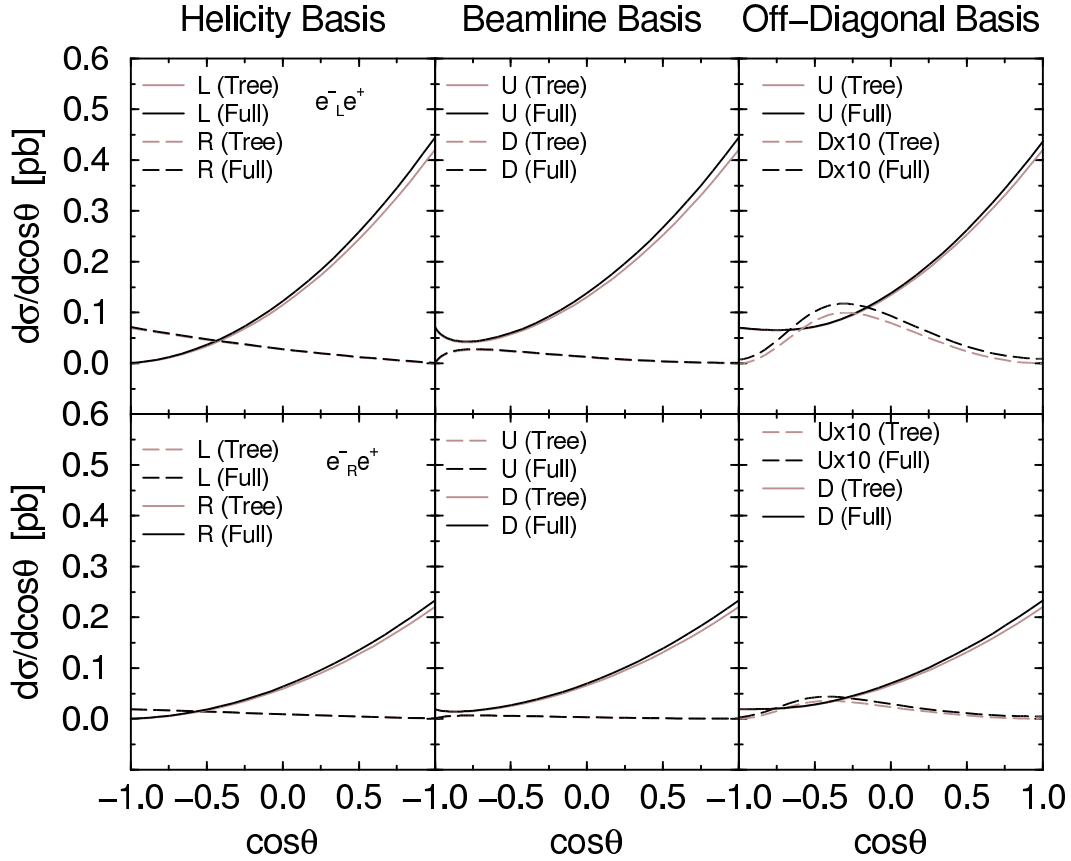


Figure 9: The cross sections in the helicity, beamline and off-diagonal bases at $\sqrt{s} = 800 \text{ GeV}$.

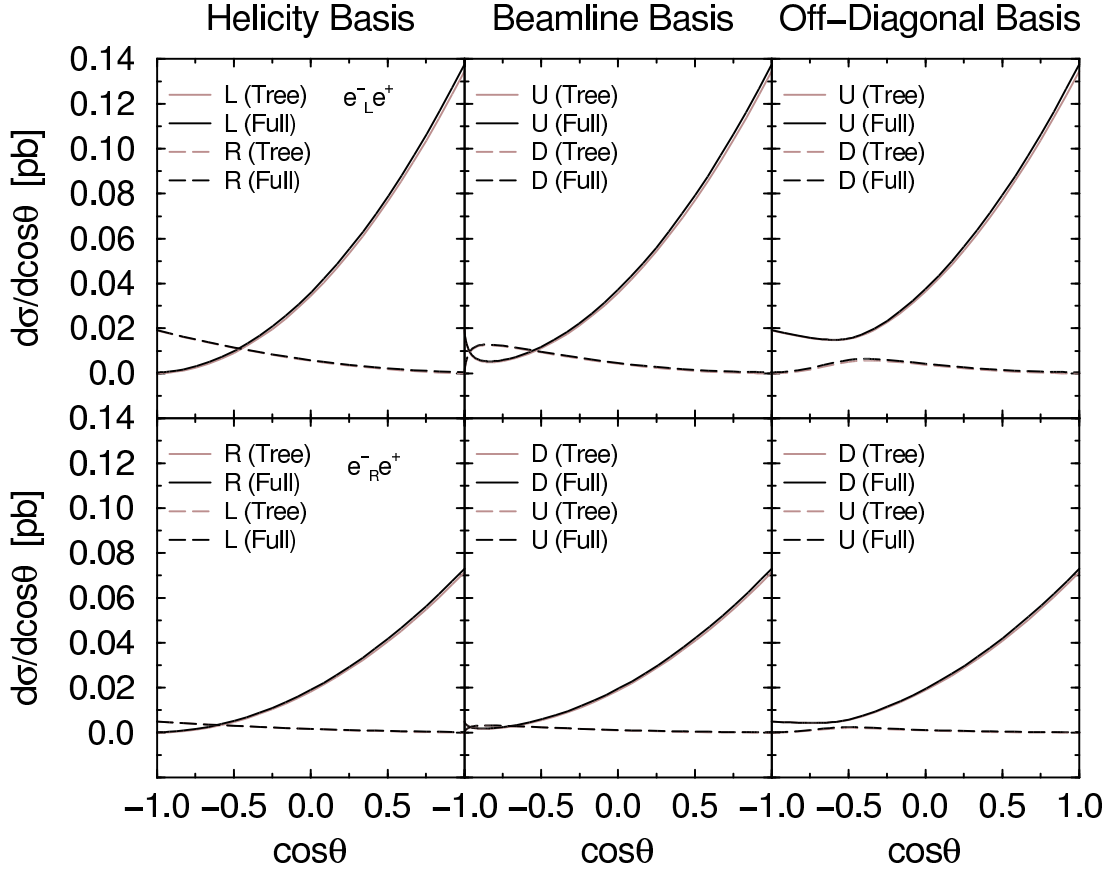


Figure 10: The cross sections in the helicity, beamline and off-diagonal bases at $\sqrt{s} = 1500$ GeV.

In Fig. 9 and 10 we have plotted the similar results for a 800 and 1500 GeV colliders. The fraction of top quarks in the dominant spin component for $e_L^- e^+$ is given in Tables 4 and 5.

$\sqrt{s} = 800$ GeV	Helicity	Beamline	Off-Diagonal
Tree	0.8318	0.9310	0.9735
$\mathcal{O}(\alpha_s)$	0.8350	0.9292	0.9682

Table 4: The fraction of the $e_L^- e^+$ cross section in the dominant spin at $\sqrt{s} = 800$ GeV for the helicity, beamline and off-diagonal bases.

$\sqrt{s} = 1500 \text{ GeV}$	Helicity	Beamline	Off-Diagonal
Tree	0.8680	0.9022	0.9535
$\mathcal{O}(\alpha_s)$	0.8671	0.8985	0.9448

Table 5: The fraction of the $e_L^- e^+$ cross section in the dominant spin at $\sqrt{s} = 1500 \text{ GeV}$ for the helicity, beamline and off-diagonal bases.

Our numerical studies demonstrate that the QCD corrections have little effect on the spin configuration of the produced top (and/or anti-top) quark for any spin basis. In particular, in the off-diagonal basis, the top (and/or anti-top) quarks are produced in an essentially unique spin configuration even after including the lowest order QCD corrections.

5 Conclusion

We have studied the $\mathcal{O}(\alpha_s)$ QCD corrections to top quark production in a generic spin basis. The QCD corrections introduce two effects not included in the Born level approximation. One is the modification of the coupling of the top and anti-top quarks to γ and Z bosons due to the virtual corrections. The another is the presence of the real gluon emission process. First, we consider the QCD corrections in the soft gluon approximation to see the effects of the modified $\gamma/Z - t - \bar{t}$ vertex. Using this approximation, we find the tree level off-diagonal basis continues to make the like spin components vanish and that the effects of the included anomalous magnetic moment are small.

Next we analyzed the full QCD corrections at one loop level. When we consider the three particle final state, the top and anti-top quarks are not necessarily produced back to back. So we have calculated the inclusive top (anti-top) quark production. In this paper we have given an exact analytic form for the differential cross section with an arbitrary orientation of the top quark spin.

Our numerical studies show that the $\mathcal{O}(\alpha_s)$ QCD corrections enhance the Born level result and only slightly modifies the spin orientation of the produced top quark. In the kinematical region where the emitted gluon has small energy, it is natural to expect that the real gluon emission effects introduce only a multiplicative correction to the Born level result. Therefore only “hard” gluon emission could possible modify the top quark spin orientation. What we have found, by explicit calculation, is that this effect is numerically very small. The size of the QCD corrections to the total cross section and the enhancement of the tree level results can be read off from the values of κ in Table 1 of Sec.4. At $\sqrt{s} = 400$ GeV, the enhancement is $\sim 30\%$ whereas at higher energies, 800 and 1500 GeV, it is at the $\sim 5\%$ level. Near the threshold, the QCD corrections have a singular behavior in β , the speed of the produced quark, this factor

enhances the value of the correction at smaller energy. The size of these corrections is reasonable for QCD, on the other hand, the change of the orientation of top quark spin are quite small. The deviation from the enhanced tree level result is less than a few percent. We can, therefore, conclude that the results of the tree level analysis are not changed even after including QCD radiative corrections except for a multiplicative enhancement. This means that for the beamline and off-diagonal bases, the top (and/or anti-top) quarks are produced in an essentially unique spin configuration. Actually, the fraction of the top quarks in the dominant (up) spin configuration for $e_L^- e$ scattering is more than 94% at all energies we have considered.

As has been discussed in many articles, there are strong correlations between the orientation of the spin of the produced top (anti-top) quark and the angular distribution of its decay products. Therefore, measuring the top quark spin orientation will give us important information on the top quark sector of the Standard Model as well as possible physics beyond the Standard Model.

Acknowledgments

The Fermi National Accelerator Laboratory is operated by the University Research Association, Inc., under contract DE-AC02-76CHO3000 with the United States of America Department of Energy. J.K. was supported in part by the Monbusho Grant-in-Aid for Scientific Research (Japan) No.C(2) 09640364. J.K. and T.N. would like to thank W. Bardeen for the hospitality extended to them at FNAL where part of this work was performed. S.P. would like to thank J. Kodaira for the hospitality extended to him while at Hiroshima University.

Appendix A : Phase space integrals over y and z

The phase space integrals necessary to derive the cross section are summarized in this Appendix. Although many of them have already appeared in the literatures [15], we will list all of them below for the convenience of the reader. After the integration over the angular variables, we are left with the following four types of integrals:

$$J_i = \int dy dz f_i(y, z), \quad N_i = \int \frac{dy dz}{\sqrt{(1-y)^2 - a}} f_i(y, z),$$

$$L_i = \int \frac{dy dz}{(1-y)^2 - a} f_i(y, z), \quad K_i = \int \frac{dy dz}{\{(1-y)^2 - a\}^{3/2}} f_i(y, z).$$

The infrared divergences are regularized by the small gluon mass λ and $\beta = \sqrt{1-a} = \sqrt{1-4m^2/s}$. For the type L_i integrals, a shorthand notation $\omega = \sqrt{(1-\sqrt{a})/(1+\sqrt{a})}$ is used. The K_i integrals have a spurious singularity at the upper bound of the y integral, $y_+ = 1 - \sqrt{a}$. Since this singularity turns out to be cancelled out in the cross section, we regularize each integrals by deforming the integration region as $y_+ \rightarrow 1 - \sqrt{a} - \epsilon$ [15]. Li_2 is the Spence function.

Class **J** Integrals:

$$J_1 = \int dy dz = \frac{1}{2}\beta \left(1 + \frac{1}{2}a\right) - \frac{1}{2}a \left(1 - \frac{1}{4}a\right) \ln \left(\frac{1+\beta}{1-\beta}\right)$$

$$J_2 = \int dy dz \frac{y}{z} = \int dy dz \frac{z}{y}$$

$$= -\frac{1}{4}\beta \left(5 - \frac{1}{2}a\right) + \frac{1}{2} \left(1 + \frac{1}{8}a^2\right) \ln \left(\frac{1+\beta}{1-\beta}\right)$$

$$J_3 = \int dy dz \frac{1}{y} = \int dy dz \frac{1}{z} = -\beta + \left(1 - \frac{1}{2}a\right) \ln \left(\frac{1+\beta}{1-\beta}\right)$$

$$J_4 = \int dy dz \frac{y}{z^2} = \int dy dz \frac{z}{y^2} = \frac{2}{a}\beta - \ln \left(\frac{1+\beta}{1-\beta}\right)$$

$$J_5 = \int dy dz \frac{1}{y^2} = \int dy dz \frac{1}{z^2}$$

$$= -\frac{2\beta}{a} \left(\ln \frac{\lambda^2}{s} + 2 \ln a - 4 \ln \beta - 4 \ln 2 + 2 \right) + 2 \left(1 - \frac{3}{a}\right) \ln \left(\frac{1+\beta}{1-\beta}\right)$$

$$\begin{aligned}
J_6 &= \int dy dz \frac{1}{yz} \\
&= \left(-\ln \frac{\lambda^2}{s} - \ln a + 4 \ln \beta + 2 \ln 2 \right) \ln \left(\frac{1+\beta}{1-\beta} \right) \\
&\quad + 2 \left[\text{Li}_2 \left(\frac{1+\beta}{2} \right) - \text{Li}_2 \left(\frac{1-\beta}{2} \right) \right] + 3 \left[\text{Li}_2 \left(-\frac{2\beta}{1-\beta} \right) - \text{Li}_2 \left(\frac{2\beta}{1+\beta} \right) \right]
\end{aligned}$$

Class N Integrals:

$$\begin{aligned}
N_1 &= \int \frac{dy dz}{\sqrt{(1-y)^2 - a}} = 1 - \sqrt{a} - \frac{1}{2} a \ln \left(\frac{2 - \sqrt{a}}{\sqrt{a}} \right) \\
N_2 &= \int \frac{dy dz}{\sqrt{(1-y)^2 - a}} \frac{z}{y} = -\frac{1}{2} \ln a + \ln(2 - \sqrt{a}) + \frac{2}{2 - \sqrt{a}} - 2 \\
N_3 &= \int \frac{dy dz}{\sqrt{(1-y)^2 - a}} \frac{y}{z} \\
&= 2\beta \ln \left(\frac{1-\beta}{1+\beta} \right) - \ln \left(\frac{1+\beta}{2} \right) \ln \left(\frac{1-\beta}{2} \right) + \left(2 - \frac{a}{2} \right) \ln \left(\frac{2 - \sqrt{a}}{\sqrt{a}} \right) \\
&\quad + \frac{1}{4} \ln^2 \frac{a}{4} - \sqrt{a} + 1 + \text{Li}_2 \left(\frac{1+\beta}{2} \right) + \text{Li}_2 \left(\frac{1-\beta}{2} \right) - 2 \text{Li}_2 \left(\frac{\sqrt{a}}{2} \right) \\
N_4 &= \int \frac{dy dz}{\sqrt{(1-y)^2 - a}} \frac{y^2}{z^2} = \frac{2}{a} (1 - \sqrt{a})^2 \\
N_5 &= \int \frac{dy dz}{\sqrt{(1-y)^2 - a}} y \\
&= \frac{1}{16} \left[-a^2 \ln a + 2a^2 \ln(2 - \sqrt{a}) + 4(2 - \sqrt{a})^2 - 4 \left(2 - a^{\frac{3}{2}} \right) \right] \\
N_6 &= \int \frac{dy dz}{\sqrt{(1-y)^2 - a}} z \\
&= \frac{1}{32} \left[12 - (2+a)^2 - \frac{2 + \sqrt{a}}{2 - \sqrt{a}} a^2 + 2(8-a)a \ln \frac{\sqrt{a}}{2 - \sqrt{a}} \right] \\
N_7 &= \int \frac{dy dz}{\sqrt{(1-y)^2 - a}} \frac{y^2}{z} \\
&= \left(1 + \frac{1}{2} a \right) \left[\text{Li}_2 \left(\frac{1+\beta}{2} \right) + \text{Li}_2 \left(\frac{1-\beta}{2} \right) - 2 \text{Li}_2 \left(\frac{1}{2} \sqrt{a} \right) + \frac{1}{4} \ln^2 \left(\frac{1}{4} a \right) \right. \\
&\quad \left. - \ln \left(\frac{1+\beta}{2} \right) \ln \left(\frac{1-\beta}{2} \right) \right] + 3v \ln \left(\frac{1-\beta}{1+\beta} \right) + \frac{1}{8} (18 + a)
\end{aligned}$$

$$\begin{aligned}
& -\frac{1}{8}(20-a)\sqrt{a} + \left(3-a + \frac{1}{16}a^2\right) \ln\left(\frac{2-\sqrt{a}}{\sqrt{a}}\right) \\
N_8 &= \int \frac{dy dz}{\sqrt{(1-y)^2-a}} \frac{1}{y} = 2 \ln\left(\frac{2-\sqrt{a}}{\sqrt{a}}\right) \\
N_9 &= \int \frac{dy dz}{\sqrt{(1-y)^2-a}} \frac{1}{z} \\
&= \text{Li}_2\left(\frac{1+\beta}{2}\right) + \text{Li}_2\left(\frac{1-\beta}{2}\right) + 2 \text{Li}_2\left(-\frac{\sqrt{a}}{2-\sqrt{a}}\right) + \frac{1}{4} \ln^2 a \\
&\quad + \ln^2\left(\frac{2-\sqrt{a}}{2}\right) - \ln(1+\beta) \ln(1-\beta) \\
N_{10} &= \int \frac{dy dz}{\sqrt{(1-y)^2-a}} \frac{y}{z^2} = \frac{4}{a} (1-\sqrt{a}) \\
N_{11} &= \int \frac{dy dz}{\sqrt{(1-y)^2-a}} \frac{1}{y^2} \\
&= \frac{2}{a} \left[-\ln \frac{\lambda^2}{s} + \ln a + 2 \ln(1-\sqrt{a}) - 4 \ln(2-\sqrt{a}) + 2 \ln 2 - 2 \right] \\
N_{12} &= \int \frac{dy dz}{\sqrt{(1-y)^2-a}} \frac{1}{z^2} \\
&= \frac{2}{a} \left[-\ln \frac{\lambda^2}{s} - \ln a + 2 \ln(1-\sqrt{a}) - \frac{1+\beta^2}{\beta} \ln\left(\frac{1+\beta}{1-\beta}\right) + 2 \ln 2 \right] \\
N_{13} &= \int \frac{dy dz}{\sqrt{(1-y)^2-a}} \frac{1}{yz} \\
&= \frac{1}{\beta} \ln\left(\frac{1-\beta}{1+\beta}\right) \left[\ln \frac{\lambda^2}{s} + \frac{1}{2} \ln a + 4 \ln(2-\sqrt{a}) - 4 \ln(2\beta) - 2 \ln\left(\frac{1-\beta}{1+\beta}\right) \right] \\
&\quad + \frac{1}{\beta} \ln^2\left(\frac{(1-\beta)^2}{\sqrt{a}(2-\sqrt{a})}\right) + \frac{2}{\beta} \ln\left(\frac{\sqrt{a}(2-\sqrt{a})}{2}\right) \ln\left(\frac{2\sqrt{a}(1-\sqrt{a})}{(1-\sqrt{a}-\beta)^2}\right) \\
&\quad + \frac{2}{\beta} \left[\text{Li}_2\left(\frac{\sqrt{a}(2-\sqrt{a})}{(1+\beta)^2}\right) - \text{Li}_2\left[\left(\frac{1-\beta}{1+\beta}\right)^2\right] + \text{Li}_2\left(\frac{(1-\beta)^2}{\sqrt{a}(2-\sqrt{a})}\right) \right] \\
&\quad + \frac{1}{\beta} \left[\text{Li}_2\left(\frac{1+\beta}{2}\right) + \text{Li}_2\left(-\frac{2\beta}{1-\beta}\right) - (\beta \rightarrow -\beta) - \frac{\pi^2}{3} \right]
\end{aligned}$$

Class **L** Integrals:

$$L_1 = \int \frac{dy dz}{(1-y)^2-a} = 2 \frac{1-a}{4-a} \ln\left(\frac{1+\beta}{1-\beta}\right)$$

$$\begin{aligned}
L_2 &= \int \frac{dy dz}{(1-y)^2 - a} \frac{z}{y} \\
&= \left(-1 + \frac{12}{4-a} - \frac{24}{(4-a)^2} \right) \ln \left(\frac{1+\beta}{1-\beta} \right) - \frac{2\beta}{4-a} \\
L_3 &= \int \frac{dy dz}{(1-y)^2 - a} \frac{y}{z} \\
&= \frac{1}{2} \ln \left(\frac{1+\beta}{1-\beta} \right) \left[\frac{1}{2} \ln a + \ln(2 + \sqrt{a}) - \ln(1 + \sqrt{a}) - 2 \ln 2 \right] \\
&\quad + \frac{1-\sqrt{a}}{\sqrt{a}} \left[\text{Li}_2(\omega) + \text{Li}_2 \left(\frac{2+\sqrt{a}}{2-\sqrt{a}} \omega \right) - (\omega \rightarrow -\omega) \right] \\
&\quad + \left[\text{Li}_2 \left(\frac{1+\omega}{2} \right) + \text{Li}_2 \left((2+\sqrt{a}) \frac{1+\omega}{4} \right) + \text{Li}_2 \left(\frac{2\sqrt{a}}{(2+\sqrt{a})(1+\omega)} \right) \right. \\
&\quad \quad \left. - (\omega \rightarrow -\omega) \right] \\
L_4 &= \int \frac{dy dz}{(1-y)^2 - a} \frac{y^2}{z^2} = \frac{2}{a} \left[\ln \left(\frac{1+\beta}{1-\beta} \right) - 2\beta \right] \\
L_5 &= \int \frac{dy dz}{(1-y)^2 - a} y = - \left(1 + \frac{1}{2}a - \frac{6}{4-a} \right) \ln \left(\frac{1+\beta}{1-\beta} \right) - \beta \\
L_6 &= \int \frac{dy dz}{(1-y)^2 - a} z = -\frac{3a}{4-a} \left(1 - \frac{2}{4-a} \right) \ln \left(\frac{1+\beta}{1-\beta} \right) + \frac{2\beta}{4-a} \\
L_7 &= \int \frac{dy dz}{(1-y)^2 - a} \frac{1}{z} = \frac{1}{\sqrt{a}} \left[\text{Li}_2(\omega) + \text{Li}_2 \left(\frac{2+\sqrt{a}}{2-\sqrt{a}} \omega \right) - (\omega \rightarrow -\omega) \right] \\
L_8 &= \int \frac{dy dz}{(1-y)^2 - a} \frac{y}{z^2} = \frac{2}{a} \ln \left(\frac{1+\beta}{1-\beta} \right)
\end{aligned}$$

Class **K** Integrals:

$$\begin{aligned}
K_1 &= \int \frac{dy dz}{\{(1-y)^2 - a\}^{3/2}} \\
&= \frac{2(1-\sqrt{a})}{\sqrt{a}(2-\sqrt{a})^2} \ln \frac{2\sqrt{a}(1-\sqrt{a})}{\epsilon(1+\sqrt{a})} - \frac{4a}{(4-a)^2} \ln \frac{(1+\sqrt{a})(2-\sqrt{a})^2}{2\sqrt{a}a} \\
K_2 &= \int \frac{dy dz}{\{(1-y)^2 - a\}^{3/2}} y \\
&= \frac{2(1-\sqrt{a})^2}{\sqrt{a}(2-\sqrt{a})^2} \ln \frac{2\sqrt{a}(1-\sqrt{a})}{\epsilon(1+\sqrt{a})} + \frac{a^2}{(4-a)^2} \ln \frac{(1+\sqrt{a})(2-\sqrt{a})^2}{2\sqrt{a}a} \\
&\quad + \ln \frac{2\sqrt{a}}{(1+\sqrt{a})}
\end{aligned}$$

$$\begin{aligned}
K_3 &= \int \frac{dy dz}{\{(1-y)^2 - a\}^{3/2}} z \\
&= \frac{2(1-\sqrt{a})^2}{(2-\sqrt{a})^3} \ln \frac{2\sqrt{a}(1-\sqrt{a})}{\epsilon(1+\sqrt{a})} + \frac{a(a^2+20a-32)}{2(4-a)^3} \ln \frac{(1+\sqrt{a})(2-\sqrt{a})^2}{2\sqrt{aa}} \\
&\quad - \frac{1}{2} \ln \frac{2\sqrt{a}}{(1+\sqrt{a})} + \frac{2a(1-\sqrt{a})}{(4-a)(2-\sqrt{a})^2} \\
K_4 &= \int \frac{dy dz}{\{(1-y)^2 - a\}^{3/2}} yz \\
&= \frac{2(1-\sqrt{a})^3}{(2-\sqrt{a})^3} \ln \frac{2\sqrt{a}(1-\sqrt{a})}{\epsilon(1+\sqrt{a})} + \frac{a^2(12-7a)}{2(4-a)^3} \ln \frac{(1+\sqrt{a})(2-\sqrt{a})^2}{2\sqrt{aa}} \\
&\quad - \frac{1}{2} \ln \frac{2\sqrt{a}}{(1+\sqrt{a})} + \frac{2}{(4-a)} \left[a \frac{(1-\sqrt{a})^2}{(2-\sqrt{a})^2} + \sqrt{a} - 1 \right] \\
K_5 &= \int \frac{dy dz}{\{(1-y)^2 - a\}^{3/2}} \frac{y}{z} \\
&= \frac{2(1-\sqrt{a})}{a(2-\sqrt{a})} \ln \frac{2\sqrt{a}(1-\sqrt{a})}{\epsilon(1+\sqrt{a})} + \frac{(4-3a)}{a(4-a)} \ln \frac{(1+\sqrt{a})(2-\sqrt{a})^2}{2\sqrt{aa}} \\
&\quad - \frac{1}{a} \ln \frac{2\sqrt{a}}{(1+\sqrt{a})} + \frac{4(1-\sqrt{a})}{a(2-\sqrt{a})} - \frac{2\beta}{a} \ln \left(\frac{1+\beta}{1-\beta} \right) \\
K_6 &= \int \frac{dy dz}{\{(1-y)^2 - a\}^{3/2}} \frac{1}{z} \\
&= \frac{2}{a(2-\sqrt{a})} \ln \frac{2\sqrt{a}(1-\sqrt{a})}{\epsilon(1+\sqrt{a})} + \frac{(4+a)}{a(4-a)} \ln \frac{(1+\sqrt{a})(2-\sqrt{a})^2}{2\sqrt{aa}} \\
&\quad - \frac{1}{a} \ln \frac{2\sqrt{a}}{(1+\sqrt{a})} + \frac{4}{a(2-\sqrt{a})} - \frac{2}{a\beta} \ln \left(\frac{1+\beta}{1-\beta} \right) \\
K_7 &= \int \frac{dy dz}{\{(1-y)^2 - a\}^{3/2}} \frac{y}{z^2} = \frac{2}{a\sqrt{a}} \ln \frac{2\sqrt{a}(1-\sqrt{a})}{\epsilon(1+\sqrt{a})} \\
K_8 &= \int \frac{dy dz}{\{(1-y)^2 - a\}^{3/2}} \frac{y^2}{z^2} \\
&= \frac{2(1-\sqrt{a})}{a\sqrt{a}} \ln \left(\frac{2\sqrt{a}(1-\sqrt{a})}{\epsilon(1+\sqrt{a})} \right) + \frac{4}{a} \ln \left(\frac{2\sqrt{a}}{1+\sqrt{a}} \right)
\end{aligned}$$

Appendix B : Total cross section

Let us examine the unpolarized total cross section including the top quark pairs using our formulae. It is given by

$$\sigma_T(\epsilon^- \epsilon^+ \rightarrow t + \bar{t} + X) = \frac{1}{4} \left[\sigma_T(\epsilon_L^- \epsilon_R^+ \rightarrow t + \bar{t} + X) + \sigma_T(\epsilon_R^- \epsilon_L^+ \rightarrow t + \bar{t} + X) \right] .$$

Note that only $k = 0, 2$ and $l, m, n = 0$ terms in Eq.(19) contribute to the total cross section. Integrating over the angle θ , we get

$$\begin{aligned} & \sigma_T(\epsilon_L^- \epsilon_R^+ \rightarrow t + \bar{t} + X) \\ &= \frac{\pi \alpha^2}{s} \beta \left[(f_{LL} + f_{LR})^2 (3 - \beta^2) \right. \\ & \quad \times \left(1 + \hat{\alpha}_s \left\{ V_I - \frac{6}{3 - \beta^2} V_{II} + \frac{2}{\beta} J_{IR}^1 - \frac{8}{\beta} J_3 + \frac{8}{\beta(3 - \beta^2)} J_2 \right\} \right) \\ & \quad + 2(f_{LL} - f_{LR})^2 \beta^2 \\ & \quad \times \left. \left(1 + \hat{\alpha}_s \left\{ V_I + 2V_{II} + \frac{2}{\beta} J_{IR}^1 - \frac{8}{\beta} J_3 + \frac{2(3 - \beta^2)}{\beta^3} J_2 + \frac{2a}{\beta^3} J_1 \right\} \right) \right] . \end{aligned}$$

The cross section for the process $\epsilon_R^- \epsilon_L^+$ is obtained by interchanging the coupling constant $L \leftrightarrow R$ in the above expression. Parametrizing the total cross section as

$$\begin{aligned} R_t(s) &\equiv \left(\frac{1}{\sigma_{\text{pt}}} \right) \sigma_T(\epsilon^- \epsilon^+ \rightarrow t + \bar{t} + X) \\ &= R_t^{(0)}(s) + \frac{\alpha_s(s)}{\pi} C_2(R) R_t^{(1)}(s) + \dots , \end{aligned}$$

where $\sigma_{\text{pt}} = 4\pi\alpha^2/3s$, we get the following numerical results at the CM energies $\sqrt{s} = 400, 500, 1500$ GeV.

\sqrt{s} (GeV)	$R_t^{(0)}(s)$	$C_2(R)R_t^{(1)}(s)$
400	1.0083	8.9963
500	1.4190	6.0267
1500	1.7714	2.2911

These are consistent with the results in Ref. [16].

References

- [1] F. Abe et al., CDF Collaboration, *Phys. Rev. Lett.* **74** (1995) 2626.
- [2] S. Abachi et al., D0 Collaboration, *Phys. Rev. Lett.* **74** (1995) 2632.
- [3] J. H. Kühn, *Nucl. Phys.* **B237** (1984) 77.
- [4] I. Bigi, Y. Dokshizer, V. Khoze, J. Kühn and P. Zerwas, *Phys. Lett.* **B181** (1986) 157.
- [5] M. Jezabek and J. H. Kühn, *Phys. Lett.* **B329** (1994) 317.
- [6] V. Barger, J. Ohnemus and R.J.N Phillips, *Int. J. Mod. Phys.* **A4** (1989) 617.
- [7] G. L. Kane, J. Pumplin and W. Repko, *Phys. Rev. Lett.* **41** (1978) 1689.
G. L. Kane, G. A. Ladinsky and C. -P. Yuan, *Phys. Rev.* **D45** (1992) 124.
- [8] M. Anselmino, P. Kroll and B. Pire, *Phys. Lett.* **B167** (1986) 113.
D. Atwood and A. Soni, *Phys. Rev.* **D45** (1992) 2405.
C. - P. Yuan, *Phys. Rev.* **D45** (1992) 318.
G. A. Ladinsky, *Phys. Rev.* **D46** (1992) 3789.
W. Bernreuther, O. Nachtmann, P. Overmann and T. Schröder, *Nucl. Phys.* **B388** (1992) 53; erratum **B406** (1993) 516.
M. E. Peskin, in *Physics and Experiments at Linear Colliders*, R. Orava, P. Eeorla and M. Nordberg, eds. (World Scientific, 1992).
T. Arens and L. M. Seghal, *Nucl. Phys.* **B393** (1993) 46.
F. Cuyper and S. D. Rindani, *Phys. Lett.* **B343** (1995) 333.
P. Poulou and S. D. Rindani, *Phys. Lett.* **B349** (1995) 379.
- [9] C. R. Schmidt and M. E. Peskin, *Phys. Rev. Lett.* **69** (1992) 410.
D. Atwood, A. Aeppli and A. Soni, *Phys. Rev. Lett.* **69** (1992) 2754.
Y. Hara, *Prog. Theo. Phys.* **86** (1991) 779.
W. Bernreuther and A. Brandenburg, *Phys. Rev.* **D49** (1994) 4481.
- [10] G. Mahlon and S. Parke, *Phys. Rev.* **D53** (1996) 4886, *Phys. Lett.* **B411** (1997) 173.

- [11] S. Parke and Y. Shadmi, *Phys. Lett.* **B387** (1996) 199.
- [12] G. Grunberg, Y. J. Ng and S. -H. H. Tye, *Phys. Rev.* **D21** (1980) 62.
J. Jersák, E. Laermann and P. Zerwas, *Phys. Rev.* **D25** (1982) 1218.
- [13] S. Groote, J. G. Körner and J. A. Leyva, hep-ph/9801255.
- [14] C. R. Schmidt, *Phys. Rev.* **D54** (1996) 3250.
- [15] S. D. Rindani and M. M. Tung, *Phys. Lett.* **B424** (1998) 125.
S. Groote, J. G. Körner and M. M. Tung, *Z. Phys.* **C70** (1996) 281.
M. M. Tung, J. Bernabeu and J. Penarrocha, *Nucl. Phys.* **B470** (1996) 41.
M. M. Tung, *Phys. Rev.* **D52** (1995) 1353.
J. G. Körner, A. Pilaftsis and M. M. Tung, *Z. Phys.* **C63** (1994) 575.
- [16] R. Harlander and M. Steinhauser, *Eur. Phys. J.* **C2** (1998) 151.